



Development of rapidly deployable instrumentation packages for data acquisition in wildland–urban interface (WUI) fires

Samuel L. Manzello*, Seul-Hyun Park, Thomas G. Cleary

Fire Research Division, Building and Fire Research Laboratory (BFRL), National Institute of Standards and Technology (NIST), Gaithersburg, MD 20899-8662, USA

ARTICLE INFO

Article history:

Received 15 April 2009

Received in revised form

8 June 2010

Accepted 24 June 2010

Available online 10 July 2010

Keywords:

Wildland–urban interface (WUI) fires

Instrumentation

Structure ignition

ABSTRACT

In an effort to quantify structure ignition mechanisms during wildland–urban interface (WUI) fires, rapidly deployable instrumentation packages were developed. For a structure under a WUI fire attack, the packages are designed to: (1) provide temporally resolved images of structure ignition mechanisms and (2) provide quantitative data on total heat flux, wind speed, wind direction, ambient temperature, and relative humidity near a structure. The unique design of the packages allowed for wireless transmission of all data signals collected to a hardened location. Prior to attempting to use these instrumentation packages in real WUI fires, a proof-of-concept test was conducted under a prescribed fire. In these tests, a shed was used as a surrogate for a typical structure that would be found in the WUI. The proof-of-concept test was successful and has demonstrated that relatively inexpensive instrumentation can be used to image structure ignition in the path of an approaching crown fire and that directional flame thermometers (DFT) were acceptable instrumentation to measure total heat flux in place of cumbersome water cooled total heat flux gages.

Published by Elsevier Ltd.

1. Introduction

The rapid growth of the wildland–urban interface (WUI) in the USA has put an increasing number of homes at risk to fires originating from wildland fuels. In the USA, there have been two significant WUI fires within the past two years in the state of California. Unfortunately, fire spread in the WUI has become an international problem as well. Recently, in 2009, fires that occurred in Victoria, Australia resulted in more than 150 fatalities and the destruction of several thousand structures.

Reduction of fire risk to WUI communities is currently handled by reducing the wildland fuel loading or by following a number of homeowner risk reduction practices (e.g. Firewise [1]). There are a variety of wildland fuel treatment methods in practice and these methods are based on very limited scientific study. As a result, the effectiveness of the various fuel treatment methods is essentially unproven and the lack of effectiveness is especially true with regard to preventing structure ignition in WUI fires. Compounding the problem of fuel treatment methods, most of the homeowner risk reduction practices follow rule-based and empirically determined checklists that lack sufficient substantiation and are not the result of a coordinated scientifically based effort [1]. Accordingly, scientific based test methods are required and need

to be tied to realistic WUI fire conditions to understand structure ignition in WUI fires.

Not surprisingly, very few full scale field experiments have been performed to understand structure ignition mechanisms [2]. Cohen [2] provided some insights into structure ignition mechanisms as part of the International Crown Fire Experiments conducted in Canada. In those experiments, Cohen [2] placed various target walls 10, 20, and 30 m from an approaching crown fire. The test walls were instrumented with Schmidt-Boelter type water cooled heat flux gages to measure the temporal evolution of heat flux experienced at a target wall as the crown fire approached. Data were obtained for seven different crown fires; three of the experiments used a dual sensor to measure both total heat flux as well as radiant heat flux. It was observed that none of the wall sections at 20 and 30 m ignited. Ignition was observed for the wall sections placed at 10 m for the approaching crown fire.

While these experiments provided some useful insights, Cohen [2] pointed out that the data were collected under a limited set of experimental conditions, such as fuel load, wind speed, and terrain. More importantly, fire spread in the WUI is not simply governed by spread from vegetative fuels to structural fuels but also from structural fuels to structural fuels. The role of firebrands during WUI fire spread is not clearly understood as well. Therefore, the capability to collect *in-situ* information on the physical mechanisms related to structure ignition during actual WUI fires is highly desirable.

NIST is developing instrumentation packages that can be used during actual WUI fires to quantify structure ignition mechanisms.

* Corresponding author. Tel.: +1 301 975 6891; fax: +1 301 975 4052.
E-mail address: samuelm@nist.gov (S.L. Manzello).

Prior to designing the instrumentation packages that are the focus of the present paper, a review of previous instrumentation packages developed to investigate wildland fire spread (not focused on structure ignition) was conducted. Although the prior instrumentation packages developed were not intended to study structure ignition, understanding the methodology developed is beneficial to guide the work presented here.

Hardy and Riggins [3] fabricated and tested field deployable packages to collect *in-situ* measurements in wildland fires. The instrumentation packages provided temporally resolved measurements of radiant and convective heat flux, horizontal and vertical airflow, air temperature, and video to image the fire behavior [3]. Similar instrumentation packages were developed to quantify fire spread in the Mediterranean region [4,5].

While the previous instrumentation packages were well thought out, the application is not the best design to consider structure ignition. First, water cooled heat flux gages are not easy to rapidly implement in field experiments. Since the desire of the NIST effort is to be able to instrument communities during actual

WUI fires, easier to setup, inexpensive measurement methods are desired since many sensors will be required to spatially resolve heat fluxes. Second, the ability to place multiple instrumentation packages and send all data wirelessly to a centrally located hardened data collection center is desired as this will greatly reduce cost and allow the construction of many remote stations that do not require extensive hardening.

To this end, instrumentation packages were designed to collect key parameters important to understand structure ignition during the WUI fires. This includes temporally resolved measurement of heat flux, wind speed, wind direction, relative humidity, ambient temperature, and full field video imaging of the structure of interest from different vantage points. It is important to point out the unique features of instrumentation developed as part of this effort. This included: (1) sending all data signal to a thermally protected hardened location (NIST WUI Black Box or Main Station) wirelessly in order to allow the use of relatively inexpensive cameras that do not need to be hardened to survive the fire and (2) quantifying heat flux without the use of water cooled heat flux

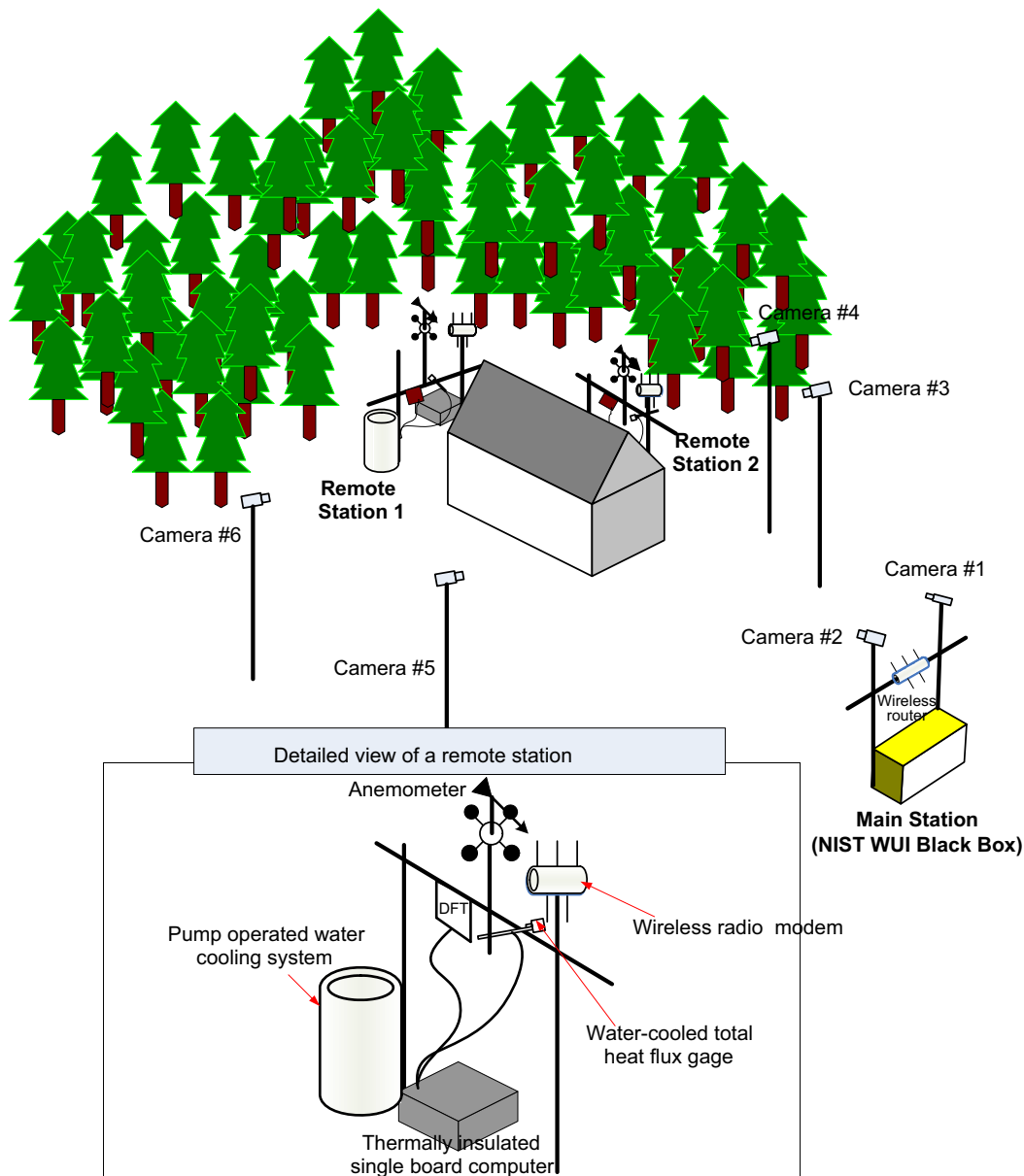


Fig. 1. Schematic of the field deployable rapid response instrumentation packages and configuration.

sensors by employing directional flame thermometers (DFT). DFT's do not require water cooling and are much easier to implement in field experimentation. Water cooled total heat flux sensors were setup to provide a direct comparison of the heat flux obtained from the DFT's.

The purpose of this study is to determine the efficacy of our instrument packages to capture shed ignition and show the danger of not implementing fuel treatments near a structure. To this end, a proof-of-concept experiment was conducted under a prescribed fire before attempting to use the instrumentation packages in real WUI fires. In these field experiments, a shed was used as a surrogate for a typical structure (that would be found in the WUI) and was intentionally placed near the vegetation to guarantee ignition. Since intense WUI fires within the USA have been observed to be wind-driven events, exposing the shed to an intense head fire was deemed as the best way to prove our concept has the potential to be used in an actual WUI fire. This paper greatly expands upon a recently presented conference publication related to NIST's efforts to develop instrumentation to quantify structure ignition [6].

2. Experimental description

Rapidly deployable instrumentation packages that collect temporally resolved measurement of heat flux, wind speed, wind direction, relative humidity, ambient temperature, as well as full field video imaging were designed. Fig. 1 displays a schematic of the field deployable rapid response instrumentation packages as well as the setup configuration used in these tests. As shown in the figure, the instrumentation packages consisted of a thermally insulated main station (NIST WUI Black Box) that was 19.5 m away from the shed and two remote stations that were placed adjacent to the shed. The dimensions of the main station (NIST WUI Black Box) were 52 cm H by 46 cm W by 64.5 cm L. The main station (NIST WUI Black Box) included a laptop with custom software for data logging, two wireless internet protocol (IP) cameras, a wireless radio modem, and a wireless router. Each remote station that faced the East and North, respectively, was equipped with single board computer (SBC) for data acquisition, a wireless radio modem, a total heat flux gage, a cup and vane anemometer, directional flame thermometer (DFT), and a temperature/humidity sensor. All instrumentation used was powered by batteries and capable of operation of more than 24 h at room temperature.

The total heat flux gages (Schmidt-Boelter type; 5/8" diameter sensor) and DFT's were used to measure the total heat flux from the fire front. Each was installed at the same height from the ground, 1.4 m, and view angle. The total heat flux gages were water-cooled during the prescribed fire and calibrated using a black body source prior to the experiments. Since there was no pressurized water available in the field, a portable water pump system was designed to provide water necessary to cool the gages. The water delivery system consisted of a positive displacement pump powered by a 12 V. The water was supplied from a 20 L container filled with 12 L of water (see Fig. 1).

A detailed schematic of the DFT is shown in Fig. 2. The DFT consisted of two 1.6 mm inconel plates which have an oxidized surface to minimize variations in surface emissivity. On the back side of each plate (facing the insulation side), K type thermocouples were welded to the center of each plate and covered with 25-mm-thick insulation material. Ambient temperature and relative humidity were measured using a temperature/humidity sensor. Local wind velocity and direction were measured using a cup and vane anemometer at the remote stations.

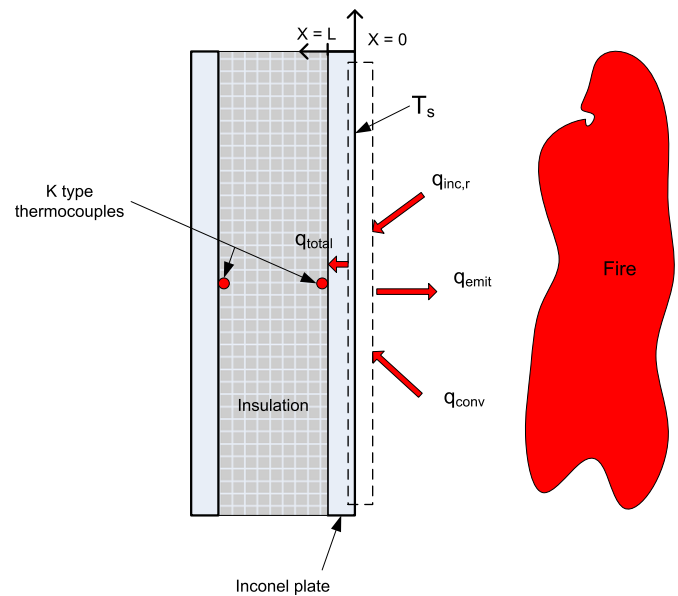


Fig. 2. Schematic of direction flame thermometer (DFT).

The SBC was located in a thermally insulated enclosure consisting of a fire safe. The SBC included eight 10 V analog input channels, and RS-232 serial ports. Additional circuitry was fabricated to provide appropriate voltage input levels from the instrumentation. DFT thermocouple voltages were amplified with cold-junction compensated type K amplifier integrated circuits as were the water cooled total heat flux gage voltages. The anemometer cup revolutions were monitored by a tachometer integrated circuit, and the vane position potentiometer and thermistor resistance were monitored with voltage divider circuits. The SBC was programmed to sample the analog inputs once a second and send the values out the serial port in a data string every second. A 900 MHz ISM frequency radio modem was connected to the serial port and transmitted the data to the main station. The main station had two companion radio modems attached to separate serial ports for point-to-point data transmission between each remote station. Fig. 3 details the data acquisition and network topography scheme.

The ability to capture temporally resolved images of structure ignition was one of the most important features of the instrumentation packages. Six expendable wireless internet protocol IP cameras, powered by batteries installed within the support poles, were installed at different view angles around the shed as well as the main station. Six cameras would clearly be sufficient to measure fire spread rate but in this study all six cameras were trained on the shed to image structure ignition mechanisms. The images were captured at 5 frames per second (fps) and simultaneously transmitted to a laptop inside the main station through a wireless router using 802.11g protocol. Commercially available IP camera monitoring software time-stamped and logged all video streams simultaneously. The corresponding images of the spreading fire front to measurement points (in terms of time) were extracted from video clips using commercial digital image processing software.

NIST was invited to test the rapidly deployable instrumentation packages by the New Jersey Forest Fire Service as part of their yearly prescribed burns intended to reduce the risk of fire spread by reducing wildland fuel loads in the New Jersey Pine Barrens. These prescribed burns were conducted at the Stafford Forge Wildlife Management Area, Warren Grove, NJ. This is land owned by the state of New Jersey. The New Jersey Forest Fire Service was

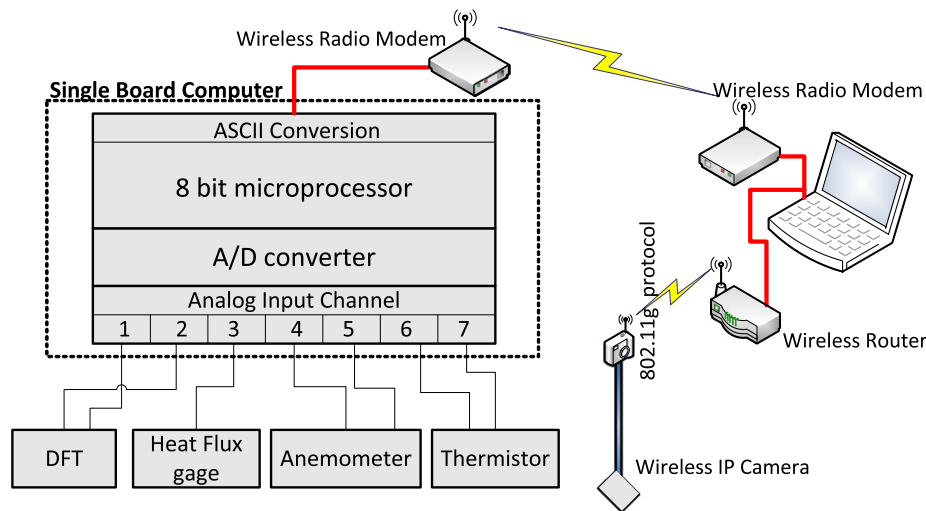


Fig. 3. Schematic of the data acquisition and network topology.

in charge of the prescribed burns which included coordination, ignition, and suppression efforts.

To visualize the ignition of the structure as the crown fire approached, a shed with dimensions of $1.8\text{ m} \times 2.4\text{ m} \times 2.0\text{ m}$ was used as a surrogate for a typical structure that would be found in the WUI. Fig. 4(a) is a picture of the shed being placed within burn site. The shed was constructed of oriented strand board (OSB) with an asphalt shingle roof and vinyl siding (see Fig. 4(b)). Fig. 5(a) displays an image of the shed in the final location prior to the fire. The cameras used can be seen in this Fig. 5(a) as well. Since these experiments were conducted to verify if the instrumentation packages would respond as designed, the shed was purposely located as close to the vegetation as possible in order to have a high likelihood of it igniting.

The fire was ignited from the air using a helicopter equipped with a heli-torch. After ignition, a crown fire developed and approached the shed with the wind (a head fire). A picture of the crown fire that developed is shown in Fig. 5(b).

3. Results and discussion

Since ignition of a given structure in the WUI is strongly dependent on the heat flux from the fire, the spread of the fire front (which is influenced by wind direction and speed, fuel load, and terrain) is an important parameter that must be quantified. In prior wildfire studies, the fire front propagation was monitored or visualized through thermocouple measurements, a series of thermally insulated CCD cameras, and infrared imaging devices [3–5]. However, high quality temporally resolved images of the fire front spread were not available in those studies.

Fig. 6(a)–(c) displays temporally resolved images of the fire approaching the structure. All instrumentation was started some four hours before the fire was ignited. The instrumentation was setup within 30 min but due to unfavorable wind, the fires were not ignited until more than four hours after setup. Ideal wind direction was necessary in order to conduct the prescribed fire in a safe manner.

Distinct fires were first observed at 4 h 5 m 28 s and propagated toward the shed with the wind. As shown in the figures, there was no evidence that the shed was ignited by: (1) firebrands or (2) radiation prior to the passage of the flame front. Since the shed was engulfed in flames upon the arrival of fire front, it is clear that direct flame impingement caused ignition of

the shed in this prescribed fire. From camera #5, shrinkage of vinyl siding on the back of the shed was observed at 4 h 6 m 20 s, before the passage of fire front. Upon the arrival of fire front, the shed was partially engulfed in the flames at 4 h 6 m 26 s. Although firebrands were not observed before the fire front attacked the shed in this prescribed fire, lofted firebrands were observed after the structure was ignited. These lofted firebrands are displayed in the Fig. 7. These images clearly show that as structures burn, firebrands produced from structures become another factor in WUI fire spread.

In addition to time resolved images of fire front and lofted firebrands, the measured ambient temperature, relative humidity, and local wind speed and direction were determined with respect to time and are shown in Figs. 8 and 9, respectively. All results were interpreted based on data obtained from the remote station #2 (approximately 0.4 m away from the shed). All data transmitted from each remote station were very similar to each other except for the heat flux data. Due to a damaged circuit that occurred at the completion of setup, the heat flux data sent to the remote computer from station #1 was meaningless. It is also important to note that all measurements were halted (at 4 h 6 m 25 s) just before the passage of fire front over the remote station because wireless communication between main and remote stations were lost. The signal loss was due to unprotected radio modems at the remote station. The SBC's survived the fire so some level of protection of the modems and antenna should extend the data transmission time.

The inverse relationship between ambient temperature and relative humidity was observed, similar to prior measurements in wildland fires [3]. The standard uncertainty in the measured relative humidity was 2% and ambient temperature was 5°C . The influence of radiative heat loss on the temperature sensor was not taken into account when reporting the ambient temperature measurements in this study. Accordingly, the uncertainty was higher for the ambient temperature measurement as the fire front approached.

As shown in Fig. 9, the local wind speed gradually decreased as the fire front approached. This may be due to the in-draft necessary to allow for continued head fire spread. The standard uncertainty in determining the wind speed was 0.5 m/s. The average wind speed for the period examined was 3.0 m/s. The wind speed information combined with video images of the fire front approaching the structure (shown in Fig. 6(a)–(c)) can provide valuable knowledge to grasp the influence of wind on WUI fires and assist firefighters on how to handle such fires. In fact, the New Jersey Forest Fire Service is using the video from these experiments: (1) for training exercises for



Fig. 4. (a) Image of the shed being placed at the burn site. (b) Details of shed interior construction are shown.

their firefighters and (2) instructional videos for homeowners as to the danger of not clearing vegetation near a home. The wind came mainly from the West and the North, fluctuating in two different directions as shown in the figure. Since the wind came from the West and the North, the fire front spread to the East as well as the South, as shown in Fig. 6(a)–(c).

To elucidate the structure ignition mechanism in WUI fires requires the temporal evolution of heat flux. In this study, the heat flux measured from both a total heat flux gage and DFT were compared in order to ascertain whether DFT's can be used in place of more cumbersome water cooled heat flux gages. DFT's do not require water cooling and have been used to quantify heat flux in fire resistance test furnaces and pool fires [7].

The measurement principal of the DFT is described. The DFT plate surface was subject to an unknown heat flux via radiative and convective heat transfer from the fire, while the temperature at $x=L$ was measured using the thermocouple with respect to time. Under these conditions, the governing one-dimensional transient heat conduction equation is given as

$$\frac{\partial^2 T}{\partial x^2} = \frac{\rho c_p}{k} \frac{\partial T}{\partial t} \quad (1)$$

$$\left. \frac{\partial T}{\partial x} \right|_{x=L} = 0 \quad (2)$$



Fig. 5. (a) Image of the shed placed at the burn site before fire; the cameras are shown. (b) Image of the prescribed fires occurred in the New Pine Barrens; the prescribed burning area was 0.1 km².

$$q(t) = -k \left. \frac{\partial T}{\partial x} \right|_{x=0} \quad (3)$$

$$T(x,0) = T_i \quad (4)$$

where T is the temperature, ρ the density of the plate, c_p the specific heat of the plate, k the thermal conductivity of the plate, and q the heat flux. This problem is referred to as an inverse heat conduction problem (IHCP) since the heat flux is obtained by

measuring the temporal variation of temperature measured at $x=L$. In the present study, the problem was solved using an IHCP solver; IHCP1D with the sequential function specification (SFS) method [8–10]. Fig. 10 displays the compensated temperature at $x=L$ of the plate of the DFT (facing the fire) as a function of time. The compensated temperature was obtained by applying a differential, dynamic error compensation technique to offset for the slow response of the sheathed thermocouples mounted behind the 1.6 mm plate of the DFT (response time of 1.9 s) [7].



Fig. 6. (a)–(c) *In-situ* temporally resolved images of fire front spread; the data loggers and cameras were started approximately four hours before the fire was ignited.

The surface heat flux history measured using the total heat flux gage and determined from the DFT are plotted as a function of time in Fig. 11. As shown in the figure, the heat fluxes increased

rapidly as the fire front approached the shed. The shrinkage of vinyl siding that covered the shed was observed at 4 h 6 m 20 s; the heat flux determined from the DFT was 25 kW/m² at this time.

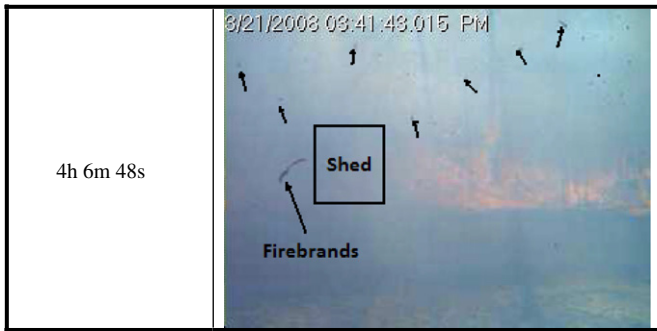


Fig. 7. Images of firebrands lofted from the structure.

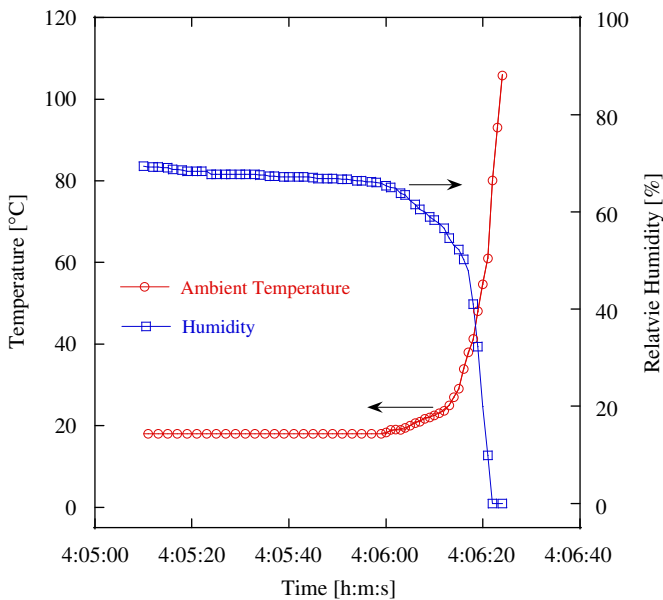


Fig. 8. Measured ambient temperature and relative humidity profiles versus time.

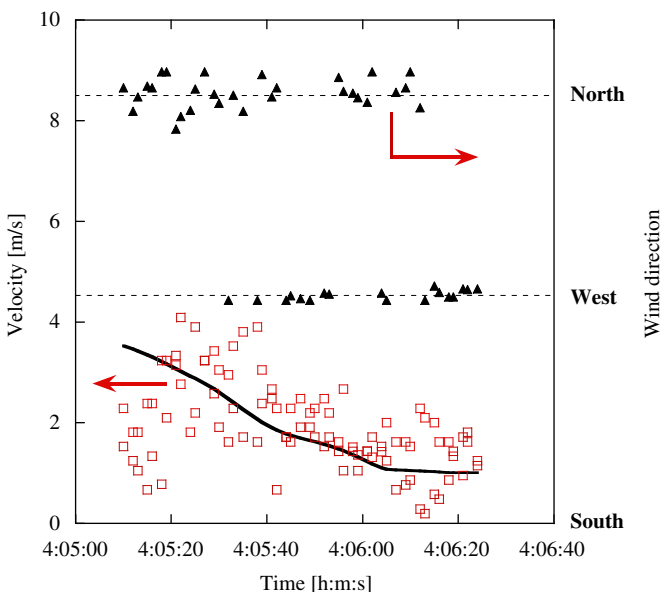


Fig. 9. Measured wind velocity and direction profiles versus time.

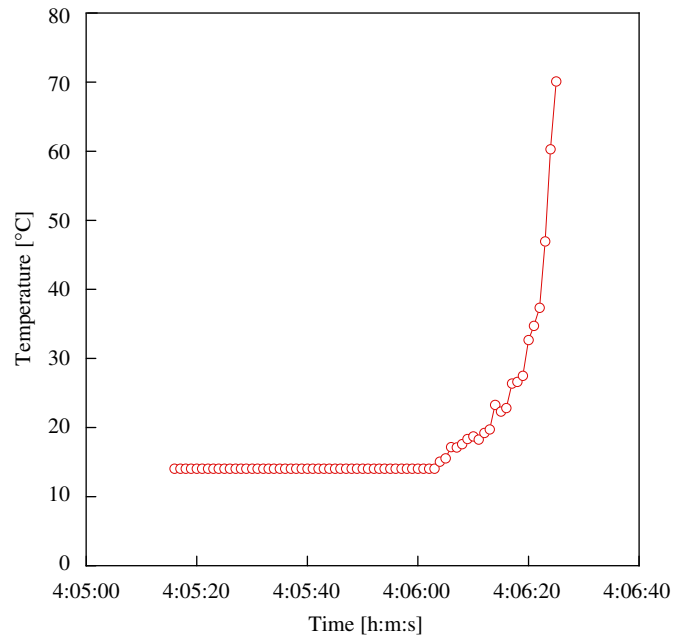


Fig. 10. Compensated temperature at $x=L$ of the plate of the DFT as a function of time.

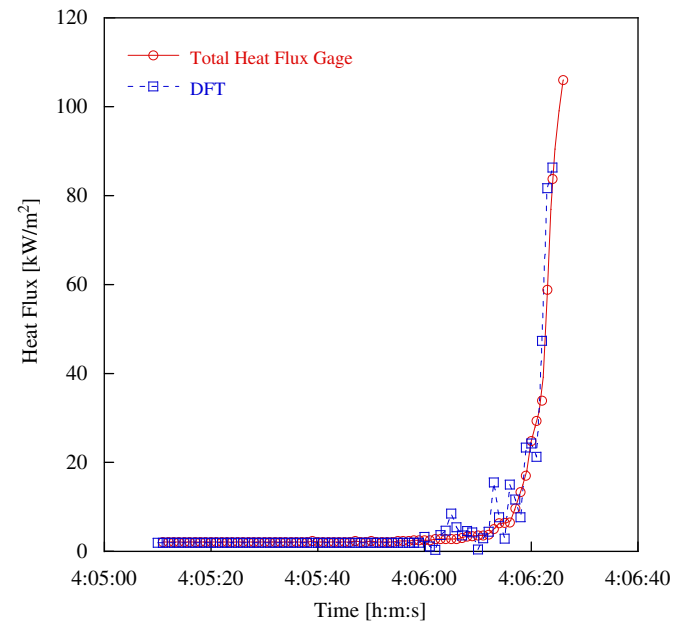


Fig. 11. Temporal variation in measured total heat flux. A comparison of water cooled total heat flux gages to DFT's is shown.

The heat flux was observed to increase to 84 kW/m² within 3 s. As can be seen in the figure, the difference in the total heat flux as measured from the DFT compared favorably to the total heat flux gages. These measurements confirm that the DFTs were acceptable for use in place of water cooled heat flux gages in characterizing heat flux from an approaching crown fire. The combined standard uncertainty in determining the total heat flux, as measured from the water cooled heat flux gages, was 10%. The main sources of certainty consisted of calibration uncertainty and uncertainty in the voltage recording process.

The combined standard uncertainty in calculating the total heat flux (using DFT's) from the IHCP method was determined.

The important parameters involved with the uncertainty evaluation include the variation in the DFT thickness, temperature measurement, thermal conductivity, and volumetric heat capacity. The individual uncertainty for the DFT thickness and temperature measurements was judged based on manufacturer specification. A 5% variation in thermal conductivity and volumetric heat capacity was applied to evaluate the uncertainty. Based on this analysis, the combined standard uncertainty in estimating the total heat flux from the inverse heat conduction method was found to be 11%. The result indicates that the largest

contributor to the combined standard uncertainty was the volumetric heat capacity followed by temperature uncertainty.

An important finding from these experiments was that the fire front passed over the shed very quickly. The shed continued to burn for more than 15 min, long after the passage of the flame front. Images of the shed burning after the passage of the fire front are displayed in Fig. 12. In real WUI fires, homes are considerably larger than the shed used and would be expected to burn for even longer duration. These results are important to understand the complexity of the fire spread problem in the WUI. The radiant heat and firebrands generated from burning structures after flame front passage can lead to ignitions of homes not immediately impacted by the main fire front, thus leading to greater losses within a community. For completeness, Fig. 13 displays the remains of the shed once burning ceased.

Future work will use instrumentation packages to quantify how effective various fuel treatment strategies are in mitigating ignition as well as placing structures further away from the vegetation to investigate firebrand ignition mechanisms. Second-generation instrumentation packages will no longer use water cooled sensors to measure heat flux; DFT's will be used. More robust methods will also be used to measure wind speed and direction.

4. Conclusions

Rapidly deployable instrumentation packages were developed to be used during actual WUI fires to quantify structure ignition mechanisms. The packages are intended to be placed near a given structure in the WUI and will provide video imaging of a structure at different vantage points as well as quantitative data on heat flux, wind speed, and relative humidity. Prior to attempting to use these instrumentation packages in real WUI fires, a proof-of-concept test was conducted under a prescribed fire. In these tests, a shed was used as a surrogate for a typical structure that would be found in the WUI.

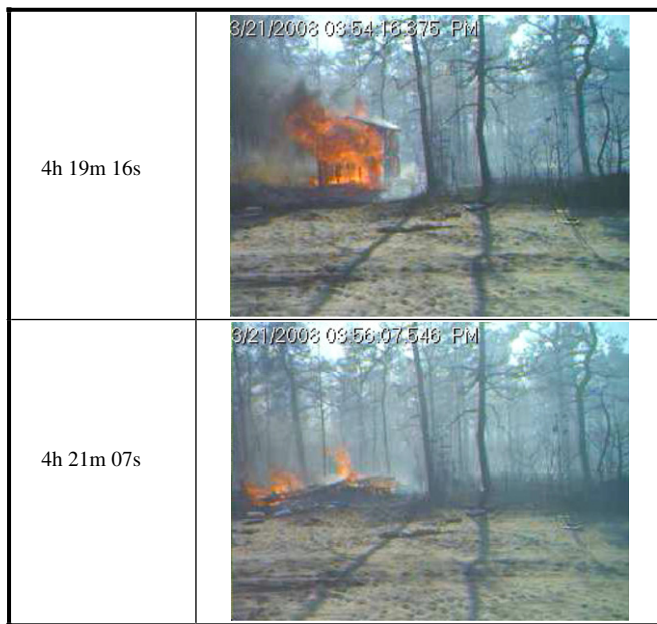


Fig. 12. Images of the shed burning long after the crown fire passed.



Fig. 13. Remains of the shed after burning ceased.

It is important to point out the unique features of instrumentation developed as part of this effort. This included: (1) sending all data signal to a hardened location (NIST WUI Black Box or Main Station) wirelessly in order to allow the use of relatively inexpensive cameras that do not need to be hardened to survive the fire and (2) quantifying heat flux without the use of water cooled heat flux sensors by employing directional flame thermometers (DFT). DFT's do not require water cooling and are much easier to implement in practice. Water cooled total heat flux sensors were used for a direct comparison of the heat flux obtained from the DFT's.

The proof-of-concept test was successful and has demonstrated that relatively inexpensive instrumentation can be used and that the DFT's are acceptable for use in place of water cooled heat flux gages. At present, the cameras were intentionally not setup to determine the rate of fire spread but were focused on imaging the shed to visualize structure ignition. In addition, characterization of the vegetation was not done as part of this study since the main thrust was to determine if the instrumentation concept delineated in this paper was feasible. However, as part of future prescribed fire studies, the vegetation will be characterized to conduct modeling studies using NIST's wildland-urban interface fire dynamics simulator (WFDS) [11] and, in conjunction with more extensive instrumentation package placement, to paint a more complete picture of fire behavior. A series of instrument packages can easily be used to determine valuable model validation data such as fire spread rate and quantitative, spatially resolved heat flux data.

The terrain plays an important role as well in fire behavior as well. The New Jersey Pine Barrens are flat as compared to mountainous areas seen in California; location of many devastating WUI fires. Differences in terrain are important and must be understood. In addition, continued work will use instrumentation packages to quantify how effective various fuel treatment strategies are in mitigating ignition as well as placing structures further away from the vegetation to investigate firebrand ignition mechanisms. Second-generation instrumentation packages will no longer use water cooled sensors to measure heat flux; DFT's will be used. More robust methods will also be used to measure wind speed and direction.

Acknowledgements

The authors are eternally grateful to the New Jersey Forest Fire Service for their gracious invitation to participate in these exciting tests. In particular, Mr. James Dusha served as the burn boss and provided incredible support to the 'NIST Science Dudes'. Mr. Stephen Maurer of the New Jersey, Forest Fire Service assisted in preparing the necessary documentation so NIST could participate. Dr. John Hom and Dr. Ken Clark of the US Forest Service are acknowledged for making us aware of this opportunity. This research was supported by the US Forest Service and Office of Science and Technology of the Department of Homeland Security. Dr. William 'Ruddy' Mell and Mr. Alexander Maranghides of NIST are acknowledged for helpful discussion and suggestions during the course of this work. Mr. John R. Shields of NIST is acknowledged assisting with the instrumentation deployment.

References

- [1] <<http://www.firewise.org>>.
- [2] J.D. Cohen, Relating flame radiation to home ignition using modeling and experimental crown fires, *Can. J. For. Res.* 34 (2004) 1161–1162.
- [3] C.C. Hardy, P.J. Riggins, Demonstration and integration of systems for fire remote sensing, ground-based fire measurement, and fire modeling, Project Final Report #JFSP-03-S-01, USDA Forest Service, 2003.
- [4] F. Morandini, et al., Fire spread experiment across Mediterranean shrub: influence of wind on flame front properties, *Fire Saf. J.* 41 (2006) 229–235.
- [5] X. Silvani, F. Morandini, Fire spread experiments in the field: Temperature and heat fluxes measurements, *Fire Saf. J.* 44 (2009) 279–285.
- [6] S.L. Manzello, et al., Developing rapid response instrumentation packages to quantify structure ignition mechanisms in wildland-urban interface (WUI) fires, in: *Proceedings of the Fire and Materials Conference*, San Francisco, CA, 2009.
- [7] N. Keltner, et al., Using directional flame thermometers for measuring thermal exposure, in: *ASTM E5—Advances in the State of the Art of Fire Testing*, Miami, FL, 2008.
- [8] W.J. Minkowycz, et al., in: *Handbook of Numerical Heat Transfer*, Wiley, 1998.
- [9] J.V. Beck, et al., in: *Inverse Heat Conduction: Ill-Posed Problems*, Wiley, 1985.
- [10] S. Chantasiriwan, Comparison of three sequential function specification algorithms for the inverse heat conduction problem, *Int. Commun. Heat Mass Transfer* 26 (1999) 115–124.
- [11] W.E. Mell, et al., Numerical simulation and experiments of burning douglas-fir trees, *Combust Flame* 156 (2009) 2023–2041.